Comparing classical and Bayesian ^{210}Pb dating models in human-impacted aquatic environments

Aquino-López, M. A., Ruiz-Fernández, A. C., Blaauw, M., & Sanchez-Cabeza, J. A. (2020). Comparing classical and Bayesian ^{210}Pb dating models in human-impacted aquatic environments. *Quaternary Geochronology*, *60*, Article 101106. https://doi.org/10.1016/j.quageo.2020.101106

Published in:
Quaternary Geochronology

Document Version:
Peer reviewed version

Queen's University Belfast - Research Portal:
Link to publication record in Queen's University Belfast Research Portal

Comparing classical and Bayesian ^{210}Pb dating models in human-impacted aquatic environments

Marco A. Aquino-López[1], Ana Carolina Ruiz-Fernández[2], Maarten Blaauw[3], Joan-Albert Sanchez-Cabeza[2]*

[1] *Maynooth University, Arts and Humanities Institute, Maynooth, Co. Kildare, Ireland.*

[2] *Unidad Académica Mazatlán, Instituto de Ciencias del Mar y Limnología, Universidad Nacional Autónoma de México, 82040 Mazatlán, México*

[3] *School of Natural and Built Environment, Queen's University Belfast, Belfast, UK.*

* Corresponding author: jasanchez@cmarl.unam.mx

Abstract

Chronologies are an essential tool to place natural archives of environmental changes on a calendar scale. Because of this, studies that compare and assess the accuracy and precision of available dating models are essential. ^{210}Pb is a radioactive isotope which is used to date recent sediments (<150 yr). Here we contrast the chronologies resulting from two different ^{210}Pb dating models: the Constant Flux model (also known as the Constant Rate of Supply model) and the recently developed Bayesian *Plum* model. This comparison was implemented by using four sediment cores from contrasting environmental settings, and showed several benefits of using a Bayesian approach. This allows to infer variables, such as the supported levels of ^{210}Pb, crucial to the chronology and commonly estimated through either samples where an asymptotic behaviour is observed or through ^{226}Ra measurements, which themselves contain some level of uncertainty. Another step of traditional methods is the selection of the equilibrium depth in order to calculate total inventories, which carries ~~out~~ strong consequences for the resulting age depth model. *Plum*, on the other hand, infers the ^{210}Pb flux, which eliminates the need to select an equilibrium depth and allows for dating cores with incomplete inventory. When traditional methods address cores with missing inventory, ^{137}Cs time markers are commonly used to correct the chronology, but *Plum* can use these time markers to improve the chronology and to reduce the uncertainty. These aspects show that the Bayesian approach results in more robust and objective chronologies, and thus in better reconstructions of environmental change over the past centuries.

Keywords: ^{210}Pb sediment dating, Bayesian Statistics, Uncertainty, Marine, Coast, Lake.

1. Introduction

Historical records of global change provide essential information to identify the main stressors affecting ecosystems. Such environmental information can feed models of potential impact scenarios and guide the development of appropriate mitigation strategies. However, because long-term instrumental records are still scarce, natural archives such as sediment cores from aquatic ecosystems that accumulate continuously, have become one of the most relevant resources of retrospective information to establish trends of environmental changes on time-scales from years to millennia or more. This information, which includes rates of change, ages of events and timing differences between records, should be based on reliable chronologies.

^{210}Pb is the most widely used radionuclide to date sediment records within the past 110-150 years, a period that includes the Anthropocene, with huge global changes associated with the need to provide food and energy resources to a rapidly growing human population (Waters et al., 2016). ^{210}Pb ($t_{½}$=22.23 years) belongs to the ^{238}U natural decay series, and its abundance in sediments ($^{210}Pb_{tot}$) results from the mixture of (a) supported ^{210}Pb ($^{210}Pb_{sup}$) produced *in situ* through the decay of ^{226}Ra in the lithosphere, and (b) excess ^{210}Pb ($^{210}Pb_{ex}$) produced after ^{222}Rn decay and transferred to sediments through dry and wet deposition, water column scavenging and runoff. Because $^{210}Pb_{ex}$ is deposited at the sediment's surface and decays over time, its activity decreases with increasing sediment depth in cores from undisturbed sediment deposits, enabling the establishment of chronologies (Appleby and Oldfield, 1992).

61 The Constant Flux (CF) model, also known as the Constant Rate of Supply
62 (CRS), (Robbins, 1978; Appleby, 1978) is a robust and widely used ^{210}Pb dating
63 model. It is based on the fundamental equation that establishes that $^{210}Pb_{ex}$ activities
64 depend on the $^{210}Pb_{ex}$ flux to the sediment surface and the sediment mass loading
65 (Krishnaswamy et al., 1971; Sanchez-Cabeza and Ruiz-Fernández, 2012). The
66 main hypothesis behind the CF model is that the $^{210}Pb_{ex}$ flux is constant, and this
67 can be used to infer estimates of temporal variations of sediment accumulation rates
68 (SAR, cm $year^{-1}$) and mass accumulation rates (MAR, g cm^{-2} $year^{-1}$). Age
69 calculations are based on the total inventory of $^{210}Pb_{ex}$ (i.e. the accumulated deposit
70 per unit area), which requires estimates of $^{210}Pb_{ex}$ data for each core section until
71 reaching the equilibrium depth (where $^{210}Pb_{tot}$ and $^{210}Pb_{sup}$ activities become
72 indistinguishable). Therefore, missing $^{210}Pb_{ex}$ data should be estimated by
73 interpolation or, in the case of cores not reaching equilibrium, missing inventory
74 extrapolated (Appleby, 2002). These restrictive requirements might cause problems
75 in sub-optimal cores (e.g., those with incomplete $^{210}Pb_{ex}$ inventory, poorly defined
76 ^{210}Pb equilibrium depth, or varying $^{210}Pb_{sup}$). Therefore, some CF-derived age-
77 models may not provide reliable chronologies, especially given the extensive global
78 land use changes that have taken place over the past century.
79 Recently, Aquino-López et al. (2018) developed a new model for ^{210}Pb dating
80 called *Plum*, which is also based on the fundamental equation and the CF
81 hypothesis. *Plum* is a Bayesian forward model that simultaneously integrates two
82 different processes: (1) the behaviour of the ^{210}Pb flux and the variation of $^{210}Pb_{sup}$
83 with depth, and (2) an age-depth function (based on *Bacon*, *a Bayesian piece-wise*
84 *linear model constrained by prior information on accumulation rate and variability*;

85 Blaauw and Christen 2011). These processes are parameterized, which allows the
86 use of a Bayesian approach. With the help of millions of Monte Carlo Markov Chain
87 (MCMC) iterations, a posterior sample can be obtained. This posterior sample
88 combines *a priori* information of sediment accumulation rates, $^{210}Pb_{ex}$ flux (typically
89 observed in a given sampling site type) and data ($^{210}Pb_{tot}$ and ^{226}Ra laboratory
90 measurements, and potentially additional information from other radioactive isotopes
91 such as ^{137}Cs and ^{14}C). Within any of the iterations, *Plum* chooses values for both
92 the age-depth function, which assigns ages to any depth, and the ^{210}Pb flux and
93 $^{210}Pb_{sup}$. With these parameters and the given ^{210}Pb's known $t_{½}$, values for $^{210}Pb_{tot}$
94 can be calculated and compared to the measurements at any depth. *Plum* only
95 requires experimental data on sediment density, $^{210}Pb_{tot}$ and ^{226}Ra activities (or at
96 least a good approximation of $^{210}Pb_{sup}$) and the outputs include estimates of $^{210}Pb_{xs}$
97 flux, supported ^{210}Pb and sediment ages. Any of these parameters are expressed
98 as posterior distributions and 95% confidence intervals.
99 In comparison to the traditional implementation of the CF model, which is a
100 reverse and deterministic model (e.g. ages are directly inferred from $^{210}Pb_{tot}$ and
101 ^{226}Ra laboratory data), *Plum* is a much more flexible forward model that allows
102 coping with non-ideal ^{210}Pb depth profiles (variable compaction poorly-defined
103 equilibrium depth). In addition, it can easily handle gaps in ^{210}Pb data or multiple
104 measurements even from the same depth, and can include other types of dating
105 information (e.g. ^{14}C dates, ^{137}Cs peak and tephras).
106 In this work, we present results of a test on the efficacy and reliability of the
107 CF and *Plum* models using data of previously published ^{210}Pb-dated sediment cores
108 from contrasting environments (deep and shallow marine areas, a crater lake, and a

109 saltmarsh) where dating difficulties were encountered. Our hypothesis was that *Plum*
110 is better than CF in managing the assumptions involved with the ^{210}Pb CF model
111 and in estimating age uncertainties. The age models obtained were contrasted with
112 stratigraphic markers (e.g. ^{137}Cs, Pu isotopes) for validation.

113 **2. Study area**

114 The sediment cores were collected from four contrasting environments in Mexico, in
115 order to reconstruct the temporal trends of a range of global change indicators
116 (Figure 1). Core IXW-500 (Ruiz-Fernández et al., 2019a) was collected from a deep-
117 sea area in the southern Gulf of Mexico (Atlantic Coast) characterized by strong
118 fluvial input, natural oil seeps, intense maritime traffic and offshore oil extraction
119 activities, and was used to assess trace metal contamination.

120 Core Tehua-II (Ruiz-Fernández et al., 2009b) was sampled from a shallow
121 marine area in the Tehuantepec Gulf (Pacific Coast) characterized by high
122 productivity associated with fluvial inputs and intense upwelling, which sustains
123 relevant commercial fisheries (e.g. tuna, shrimp and shark) and experiences strong
124 shipping traffic owing to oil production and distribution activities. For this core,
125 temporal variations of sediment accumulation rates were determined in order to
126 reconstruct land use changes.

127 Core AIII (Ruiz-Fernández et al., 2016) was sampled to estimate rates of sea
128 level rise at a saltmarsh in Estero de Urías (Gulf of California, Pacific Coast) an
129 anthropized lagoon that hosts a harbour with shipping activities ranging from
130 cabotage and fishing (mainly tuna and shrimp) to passenger cruises, and which also
131 receives untreated domestic and industrial wastes.

Finally, core SAMO2014-2 (Ruiz-Fernández et al., 2019b) was collected to determine mass accumulation rates in Lake Santa Maria del Oro, a 2-km diameter and 65m deep oligomictic and mesotrophic crater lake (Cardoso-Mohedano et al., 2019). The lake is mainly used for recreational activities, and it is located within the Trans-Mexican Volcanic Belt at 65 km from the Pacific Coast.

3. Methods

The sediment cores were collected with transparent PVC tubes of different internal diameter and assisted by different types of samplers (see Table 1 for sampling details). The cores were extruded and cut into contiguous 1 cm thick sections. Samples were weighed before and after freeze-drying; sediment bulk density (g cm^{-3}) was calculated as the ratio of the total dry mass and the volume (from diameter and thickness) of each core section.

3.1. Laboratory analysis

All sediment cores were analysed in the Sediment Dating Academic Service at UNAM, following the methodology described in previous publications (Ruiz-Fernández et al., 2009, 2016, 2019a, 2019b). To summarise, $^{210}Pb_{tot}$ activities were measured using alpha spectrometry (Alpha Ensemble Ortec/Ametek) according to Ruiz-Fernández and Hillaire-Marcel (2009). $^{210}Pb_{sup}$ activities were estimated using gamma spectrometry measurements of ^{226}Ra activities (through its daughter radionuclide ^{214}Pb, 352 keV) using a low-background Ortec HPGe well-detector (Ruiz-Fernández et al., 2014). $^{210}Pb_{xs}$ activities were determined using the difference between $^{210}Pb_{tot}$ and $^{210}Pb_{sup}$ activities. To validate the ^{210}Pb-derived chronologies, the activity profiles of ^{137}Cs against depth were determined by gamma-ray spectrometry (662 keV) in all cores, and plutonium isotopes were determined by i)

156 alpha-particle spectrometry for core SAMO14-2 (Ruiz-Fernández et al., 2019b), ii)
157 low-energy accelerator mass spectrometry for core EUIII (in Centro Nacional de
158 Aceleradores, Spain; Ruiz-Fernández et al., 2016) and iii) mass spectrometry in
159 Spiez Laboratory (Switzerland) for core IXW-500.

160 *3.2. ^{210}Pb-derived chronologies*

161 In the original papers, chronologies, mass and sediment accumulation rates were
162 estimated with the constant flux (CF) model (Appleby and Oldfield, 1978; Robbins,
163 1978; Sanchez-Cabeza and Ruiz-Fernández, 2012). Dating uncertainties in core
164 Tehua-II were calculated using quadratic propagation uncertainty, whereas in the
165 other cores they were estimated by Monte Carlo simulation with 10^5 simulations
166 (Sanchez-Cabeza et al., 2014).

167 The *Plum* age-depth models were obtained using the default settings. These
168 settings dictate the prior distributions used for the supported ^{210}Pb, ^{210}Pb flux, and
169 sedimentation rate and its variability (used within each *Bacon* section), as well as
170 the thickness of *Bacon* sections. By default, *Plum* uses 1-cm thick *Bacon* sections
171 (whereas *Bacon*'s default is 5, which is probably too restrictive to model
172 sedimentation close to the surface). The default prior distribution for the supported
173 ^{210}Pb parameters is a gamma distribution with a mean of 15 Bq kg^{-1} and a shape
174 parameter of 2. For core IXW500, *Plum* used the ^{226}Ra measurements to obtain
175 estimates for supported ^{210}Pb at multiple depths, whereas for the other cores
176 supported ^{210}Pb was assumed to be constant throughout each core. For the ^{210}Pb
177 flux, *Plum* uses a gamma distribution with a mean of 50 Bq m^{-2} yr^{-1} and a shape
178 parameter of 2. *Plum* also uses an upper age limit, for which it uses a parameter set
179 to A_I=0.1 by default, which is defined as the remaining unmeasured $^{210}Pb_{ex}$. This

180 variable allows for faster convergence of the MCMC, and limits the chronology
181 according to the inferred $^{210}Pb_{ex}$ flux. *Plum* also can use information from time-
182 markers such as the human-made peak in ^{137}Cs to refine the age-depth model, but
183 this was ignored as we wanted to observe only the behaviour of the ^{210}Pb data on
184 their own.

185 **4. Results**

186 Figures 2, 3, 4 and 5 show the comparisons between the ^{210}Pb-derived chronologies
187 using the CF and *Plum* dating models.

188 *4.1. TEHUA-II*

189 In the case of TEHUA-II (Figure 2), both models agreed well with each other
190 throughout the chronologies. The CF confidence intervals overlapped *Plum*'s
191 credible intervals, i.e. *Plum* provided narrower intervals. In this case, *Plum* was able
192 to extend the chronology by up to two decades, because fewer measurements were
193 discarded in order to infer the supported ^{210}Pb. Both models agreed quite well with
194 the 1963 time-marker.

195 *4.2. EU-III*

196 Figure 3 shows the comparison between the *CF* and *Plum* age-models of core EU-
197 III. In this case, the chronologies agreed well with each other, providing similar age
198 estimates and similar credible and confidence intervals. Again, *Plum* was able to
199 extend the chronology for several decades as several more data points are used to
200 infer the chronology: CF inferred a chronology up to a depth of 27.5 cm, whereas
201 *Plum* reached a depth of 39 cm. Regarding the 1963 time marker, *Plum* seems to
202 agree better as the CF model provided younger ages and its uncertainty was
203 insufficient to enclose the time marker.

204 *4.3. SAMO14-2*

205 SAMO14-2's chronology (Figure 4) showed that the age estimates are in good
206 agreement and both models enclose the time marker within its intervals. On the other
207 hand, the model's uncertainty estimates show largeed differences, with *Plum*
208 providing more conservative uncertainty estimates. Regarding the length of the
209 chronology, *Plum* was again able to extend the chronology by several decades by
210 its use of fewer measurements to infer the supported ^{210}Pb value.

211 *4.4. IXW-500*

212 In this case, the CF- and *Plum*- derived age models resulted in significant differences
213 (Fig. 5) at different core depths. In comparison with CF ages, *Plum* ages were older
214 in the segments surface – 4 cm and 8 – 12 cm, but comparable within the segments
215 5 – 8 cm and below 12 cm. *Plum* provided a more conservative age estimate, with
216 larger and more credible intervals than the CF model. In this particular case, The
217 *Plum*-derived age model comprised almost twice the CF age period (age estimate
218 of 160 years at 15 cm depth and 308 years at 29 cm depth). This was caused by CF
219 having to discard the 5 bottom measurements, whereas *Plum* was able to extract
220 information from them.

221 The considerable differences between the models could be caused by the
222 peculiar ^{226}Ra profile of this core (shown as blue dots in the supported ^{210}Pb panel
223 in Figure 4). The largest difference between the age models was observed at mid-
224 depth, where a minimum $^{210}Pb_{ex}$ in activity occurs, caused by large ^{226}Ra activity.
225 This also resulted in both models presenting a change in behaviour at this depth,
226 with a larger accumulation rate at depths lower than 9 cm. In this case, refining the
227 chronology using more information (e.g. ^{137}Cs) could be of help, as *Plum* can include

these time markers to the likelihood function in order to obtain an integrated chronology.

It is important to note that both total ^{210}Pb and ^{226}Ra at the five deepest samples were very similar, i.e. equilibrium was reached. In this case, *Plum* uses the information provided by the rest of the core and the prior distribution to provide an informed extrapolation.

5. Discussion

5.1. Tehua-II and EU-III

As all sections of these cores were measured down to equilibrium, as expected both models provided similar results. In the case of TEHUA-II, *Plum* provided narrower credible intervals, which are a result of the use of the *Bacon* age-depth function, instead of the decay equation used by the CF model. On the other hand, the age-models for EU-III agreed well and reconstructed similar uncertainty intervals. *Plum* was able to extend the chronology by a couple of decades in the case of TEHUAII and by more than 100 yr in the case of EU-III. This is a result of *Plum*'s integration of supported ^{210}Pb in the inference process, removing the need to discard the lowermost few measurements.

5.2. SAMO14-2

SAMO14-2 presents an interesting case as relatively few data points were available for the inference. Both models presented overlapping results. In this case, *Plum* provided wider intervals as a result of the low number of samples measured for this core. The CF model provided very precise age estimates, apparently a positive outcome, but considering that less than 25% of the core sections were measured (10 measurements of 1 cm sections were used to infer the chronology to a depth of

41 cm), the more conservative intervals provided by *Plum* are more coherent. This is an important consequence of the interpolations used to estimate the $^{210}Pb_{ex}$ inventories, which do not consider the error caused by the absence of measurements. Interestingly, something similar appears to happen in simulated and real-world ^{14}C-dated cores modelled using classical and Bayesian age-models (Blaauw et al. 2018): whereas Bayesian age-models become more precise with increasing dating densities (they 'learn'), classical age-models such as linear interpolation do not.

5.3. IXW-500

This core presented significant differences between each model. *Plum* inferred lower levels of supported ^{210}Pb at 8 – 10 cm depths in comparison to the measured ^{226}Ra (see Figure 5). It is at these depths where both models show their largest discrepancies. In this case, more measurements around the spike of ^{226}Ra could help *Plum* to model these unusual spikes. Also, *Plum* can use other time markers such as ^{137}Cs to refine the chronology.

5.4. Plum extended chronologies

As shown, *Plum* is able to obtain longer chronologies. In some cases, the extension is a result of fewer samples being used exclusively to infer supported ^{210}Pb and/or the use of the final sample with $^{210}Pb_{ex}$ not being discarded (which is common practice when using the CF model). These extensions provide an accurate chronology with an uncertainty similar to the rest of the chronology. In other cases, like IXW-500, it is the result of using ^{226}Ra concentrations combined with a sediment with ^{210}Pb in equilibrium. *Plum* provides a much larger extension in these chronologies, but this should be taken with extra caution, since at depths below

where $^{210}Pb_{ex}$ is available, age uncertainties become considerably higher and precision decreases. These extensions are a linear simplification, which uses information from both the data and the prior distributions for the accumulation rate and variability. Under simulation, we have observed that these extensions become more inaccurate with depth, but the credible intervals (larger than in the rest of the chronology) are able to capture the true age. These extensions are rather qualitative and should not be used to obtain conclusions on sedimentary processes and records. Because simulations are not within the scope of the present study, these are left for future research.

~~As shown, Plum is able to obtain longer chronologies. In some cases, the extension is a result of fewer samples being used exclusively to infer supported 210Pb and/or the use of the final sample with 210Pbex not being discarded (which is common practice when using the CF model). These extensions provide an accurate chronology with an uncertainty similar to the rest of the chronology. In other cases, like IXW-500, it is the result of using 226Ra concentrations combined with a sediment with 210Pb in equilibrium. Plum provides a much larger extension in these chronologies, but this should be taken with caution. These extensions are a linear simplification, which uses information from both data and the prior distribution for the accumulation rate. Under simulation, we have observed that these extensions become more inaccurate with depth, but the credible intervals (larger than in the rest of the chronology) are able to capture the true age. These extensions are rather qualitative and should not be used to obtain conclusions on sedimentary processes and records~~

299 *5.5. CF rapid accumulation*

300 The CF model was constructed using the decay equation as its basis, which resulted
301 in a logarithmic age-depth function; $t(x) = \lambda^{-1} log\left(\frac{A(0)}{A(x)}\right)$. This age-depth function
302 works well in the most recent part of the sediment, but as the remaining activity $A(x)$
303 gets close to 0, the age function rapidly tends to infinity, resulting in an artificial
304 increase of accumulation rates. This increase is not caused by natural sources but
305 it is a result of the mathematical structure of the model and should not be included
306 in interpretations. On the other hand, because *Plum* uses an independent age-depth
307 function, it does not show this artificial increase in accumulation, providing a more
308 realistic age-depth function at deeper parts of the sediment.

309 *5.6. Overall considerations*

310 When CF model users are confronted with a new core, a number of decisions must
311 be made based on the available information. Because of resource constraints,
312 typically not all core sections are measured and interpolation techniques are needed,
313 which may induce an experimental error. By design, *Plum* does not need any kind
314 of interpolation and solely relies on the existing data. While both the CF model and
315 *Plum* should produce better age-models with more data (i.e. more information), *Plum*
316 results are undoubtedly more reliable when some data are missing.

317 The reliability of measurement can also be sometimes an issue. For example,
318 the CF radiochronologist might decide that a measurement is an outlier, or that
319 concentrations close or below 0 Bq kg^{-1} are zero. In the case of *Plum*, this is not an
320 issue, as the system will choose, based on Bayesian statistics, which is the best set

of activities and, in some cases, disregard an outlier or ignore low (or negative) concentrations, without human intervention.

One of the critical decisions that must be taken when using the CF model is the selection of the equilibrium depth of the core, i.e., the depth where the $^{210}Pb_{ex}$ reaches zero and from where the total $^{210}Pb_{ex}$ inventory can be calculated. The equilibrium depth mainly depends on the unambiguous knowledge of the $^{210}Pb_{sup}$ value. This is often difficult to ascertain owing to i) large relative uncertainties of $^{210}Pb_{ex}$, when calculated by subtraction of ^{210}Pb and ^{226}Ra (or an estimated $^{210}Pb_{sup}$), which can be very similar at the core bottom, and ii) changes in sediment composition which can produce variations of $^{210}Pb_{sup}$ activities along a core (e.g. Carnero-Bravo et al. 2016), which will affect the total $^{210}Pb_{xs}$ inventory and thus the core age, as higher inventories will cause younger ages and vice versa. Therefore, depending on the core's ^{210}Pb activity profile, small variations of specific activities could produce age variations amounting to decades. A relevant feature of *Plum* is that $^{210}Pb_{sup}$ is not a a value to be provided by the user ~~user's input~~ but a parameter to be inferred. *Plum* uses data to infer $^{210}Pb_{sup}$, which can be ^{226}Ra measurements or ^{210}Pb which reached equilibrium. If only ^{210}Pb is available, *Plum* runs a pre-analysis based on a linear regression, where the segment which provides the largest p-value (and thus lower variability) is suggested to be used exclusively to infer $^{210}Pb_{sup}$. Because the p-value is affected by sample size, this pre-analysis should be confirmed by the user, but it has provided reasonable results in several simulations and real cores. This reduces considerably the calculation efforts and decisions of the user, and maximizes the confidence in the $^{210}Pb_{sup}$ value.

Sometimes the ^{210}Pb profile is incomplete, i.e. ^{210}Pb does not reach equilibrium. In this case, CF users need to estimate the missing inventory from either a bottom constant accumulation rate, or by using a reference date (e.g. the ^{137}Cs maximum). In the case of *Plum* this is not needed, as even in these cases *Plum* will estimate the total $^{210}Pb_{ex}$ flux by Bayesian statistics.

In overall, these and other decisions may cause different scientists, or even the same scientist at different moments, to produce different chronologies with the same data set and using the same model. As *Plum* uses existing information, age models should be identical (as long as the prior parameters are the same) and the user-based bias should largely reduced. In this sense, *Plum* is clearly more objective and we suggest that it should be widely used by ^{210}Pb radiochronologists.

~~*Plum* produces ^{210}Pb-chronologies up the maximum core length (Fig. 5) based on the assumption that mass accumulation rates (g cm^{-2} yr^{-1}) are constant beyond the core section from where $^{210}Pb_{ex}$ is available and using both data from the most recent part of the sediment and the prior distribution. This is a useful *Plum* feature allowing practical applications (e.g. selection of core sections from pre-industrial times, a rough estimation of the maximum core age, correlation among core sections). However, caution is advised when using these extrapolated ages beyond where $^{210}Pb_{ex}$ is available, since age uncertainties become considerably higher and precision decreases. The behaviour of these extensions can only be analysed with help of simulations. Because simulations are not within the scope of this study, these are left for a future study.~~

In this comparison study, only ^{210}Pb measurements were used to produce chronologies. However, for core IXW-500 additional nuclides were measured,

368 including ^{137}Cs, which has known historical peaks caused by radioactive releases
369 into the atmosphere. Such peaks are regularly used to validate or adjust ^{210}Pb-based
370 chronologies. *Plum* can integrate such information, as well as ^{14}C and other dates,
371 into the ^{210}Pb chronology.

372 **6. Conclusions**

373 The application of the CF ^{210}Pb sediment dating model requires from the
374 radiochronologist several inputs, such as the equilibrium depth and data
375 interpolation when not all sections are measured, a rather common case. However,
376 with the Bayesian approach used by *Plum* this is no longer needed, thus making the
377 dating process less subjective and more reproducible.

378 The comparison of both approaches show that *Plum* provides similar results
379 to the classical CF model, with the added benefits of providing more precise
380 uncertainty estimates when sampling density is high (like in the case of TEHUA-II
381 and EU-III), and providing more realistic uncertainty estimates where few samples
382 are available (SAMO14-2). Also, *Plum* is not affected by artificial increases of
383 sedimentation in the deepest part of the sediment, unlike the CF model where the
384 logarithmic age-function tends to infinity as background is reached. This allows the
385 user to interpret dates deeper in the core without being affected by artificial increases
386 in the sedimentation.

387 *Plum'* older ages, obtained by the usability of more data, appears to be in
388 disagreement with previous chronology limits (Appleby, 1998). This point was
389 previously addressed by Aquino-López el at. (2018), as by using simulations it was
390 shown that these older ages remained accurate when the core is fully sampled.
391 These older ages are also accompanied by a more realistic uncertainty (much larger

credible intervals), and should be handled with caution, even more when the core was is not fully sampled. Users and/or studies which required less uncertainty should consider discarding these older ages or providing the model with other time markers, which will improve the levels of uncertainty and help the model provide a more precise chronology.

The ability of adding extra information such as ^{137}Cs, radiocarbon dates and/or tephra dates can be used for both validating the chronology or improving it. Because *Plum* uses raw ^{210}Pb to create the chronology, multiple isotope chronologies are possible without having to pre-model the ^{210}Pb dates. This quality should not be underestimated, as the effects of the bias in the deepest part of the sediment presented by the CF model have not yet been studied. Because of all these considerations, we believe that *Plum* has the potential of providing more robust and objective ^{210}Pb chronologies.

Acknowledgements

The authors acknowledge partial financial support from a Royal Society-Newton Mobility Grant (Dating the decadal-scale dynamics of ENSO and pollution trends from crater lake sediments in Nayarit, western tropical Mexico), CONACYT (PDCPN 2015-01/473, CONACYT-CNR C0013-2016-05-277942, SEMARNAT-2016-01-278634), UNAM (PAPIIT IN110518 and IN104718; LANCAD-UNAM-DGTIC-273). Part of this work was funded by a CONACYT postgraduate scholarship 411036 to Marco A. Aquino-López at Queen's University Belfast. Authors are grateful to the technical support received by L.H. Pérez-Bernal, León Felipe Álvarez, H. Bojórquez-Leyva, S. Rendón-Rodríguez, G. Ramírez Reséndiz and C. Suárez-Gutiérrez.

Data Availability

Sediment data are available as supplementary material.

Supplementary material

- Data used for ^{210}Pb dating with *Plum*.

References

Appleby, P. G., Oldfield, F. (1978). The calculation of lead-210 dates assuming a constant rate of supply of unsupported ^{210}Pb to the sediment. Catena, 5(1), 1-8.

Appleby, P. G., Oldfield, F. (1992). Application of lead-210 to sedimentation studies. Uranium-Series Disequilibrium: Applications to Earth, Marine, and Environmental Sciences, 2nd edition. Oxford: Clarendon, 731-778.

Appleby, P. G. (1998). Dating recent sediments by 210Pb: Problems and solutions. Proc. 2nd NKS/EKO-1 Seminar, Helsinki, 2-4 April 1997, STUK, Helsinki, pages 7–24.

Appleby, P. G. (2002). Chronostratigraphic techniques in recent sediments. In Tracking environmental change using lake sediments (pp. 171-203). Springer, Dordrecht.

Aquino-López, M. A., Blaauw, M., Christen, J. A., Sanderson, N. K. (2018). Bayesian analysis of ^{210}Pb dating. *Journal of Agricultural, Biological and Environmental Statistics*, 23(3), 317-333.

Blaauw, M. Christen, J. A. (2011). Flexible paleoclimate age-depth models using an autoregressive gamma process. *Bayesian Analysis*, 6(3), 457-474.

Blaauw, M., Christen, J.A., Bennett, K.D., Reimer, P.J., 2018. Double the dates and go for Bayes – impacts of model choice, dating density and quality on chronologies. *Quaternary Science Reviews*, 188, 58—66

440 Cardoso-Mohedano, J. G., Sanchez-Cabeza, J. A., Ruiz-Fernández, A. C., Pérez-
441 Bernal, L. H., Lima-Rego, J., Giralt, S. (2019). Fast deep water warming of a
442 subtropical crater lake. *Science of the Total Environment*, 691, 1353-1361.
443 Carnero-Bravo, V., Sanchez-Cabeza, J. A., Ruiz-Fernández, A. C., Merino-Ibarra,
444 M., Hillaire-Marcel, C., Corcho-Alvarado, J. A., Röllin, S., Diaz-Asencio, M.,
445 Cardoso-Mohedano, J.G., & Zavala-Hidalgo, J. (2016). Sedimentary records of
446 recent sea level rise and acceleration in the Yucatan Peninsula. *Science of the*
447 *Total Environment*, 573, 1063-1069.
448 Krishnaswamy, S., Lal, D., Martin, J., Meybeck, M. (1971). Geochronology of Lake
449 Sediments. *Earth and Planetary Science Letters* 11: 407–14.
450 Robbins J. A. (1978) Geochemical and geophysical applications of radioactive lead
451 isotopes. In Biochemistry of Lead (ed. J. O. Nriagu). Elsevier, Amsterdam, pp.
452 85–393.
453 Ruiz-Fernández A.C., Hillaire-Marcel C. (2009a). ^{210}Pb-derived ages for the
454 reconstruction of terrestrial contaminant history into the Mexican Pacific coast:
455 Potential and limitations. *Marine Pollution Bulletin* 59, 134–145.
456 Ruiz-Fernández A. C., Hillaire-Marcel C., de Vernal A., Machain-Castillo M. L.,
457 Vásquez L., Ghaleb B., Aspiazu-Fabián, J.A., Páez-Osuna F. (2009b).
458 Changes of coastal sedimentation in the Gulf of Tehuantepec, South Pacific
459 Mexico, over the last 100 years from short-lived radionuclide measurements.
460 *Estuarine Coastal and Shelf Science* 82, 525–536.
461 Ruiz-Fernández, A. C., Maanan, M., Sanchez-Cabeza, J. A., Pérez-Bernal, L. H.,
462 López-Mendoza, P., Limoges, A. (2014). Chronology of recent sedimentation

463 and geochemical characteristics of sediments in Alvarado Lagoon, Veracruz
464 (southwestern gulf of Mexico). Ciencias Marinas, 40(4), 291-303.
465 Ruiz-Fernández A. C., Sanchez-Cabeza J. A., Serrato de la Peña J. L., Perez-Bernal
466 L. H., Cearreta, A., Flores-Verdugo F., M. L. Machain-Castillo, Chamizo E.,
467 García-Tenorio R., Queralt I., Dunbar R. B., Mucciarone D.A., Diaz-Asencio M.
468 (2016). Accretion rates in coastal wetlands of the southeastern Gulf of
469 California and their relationship with sea level rise. *The Holocene* 26, 7, 1126–
470 1137.
471 Ruiz-Fernández A.C., Sanchez-Cabeza J.A., Pérez-Bernal L. H., Gracia-Gasca A.
472 (2019a). Spatial and temporal distribution of heavy metal concentrations and
473 enrichment in the Southern Gulf of Mexico. *The Science of the Total*
474 *Environment 651*, Part 2, 3174-3186.
475 Ruiz-Fernández A.C., Sanchez-Cabeza J. A., Hernández-Rivera D.M., Pérez-Bernal
476 L. H., Cardoso-Mohedano J. G. (2019b). Historical reconstruction of sediment
477 accumulation rates as an indicator of global change impacts in a tropical crater
478 lake in Mexico. *In preparation.*
479 Sanchez-Cabeza J.A., Ruiz-Fernández A.C. (2012). ^{210}Pb sediment
480 radiochronology: an integrated formulation and classification of dating models.
481 *Geochimica et Cosmochimica Acta* 82, 183–200.
482 Sanchez-Cabeza J. A., Ruiz-Fernández AC, Ontiveros Cuadras JF, Pérez Bernal
483 LH, Olid C (2014). Monte Carlo uncertainty calculation of ^{210}Pb chronologies
484 and accumulation rates of sediments and peat bogs. *Quaternary*
485 *Geochronology* 23, 80–93

Waters, C. N., Zalasiewicz, J., Summerhayes, C., Barnosky, A. D., Poirier, C., Gałuszka, A., Cearreta, A., Edgeworth, M., Ellis, E.C., Ellis, M., Jeandel, C., Leinfelder, R., McNeill, J. R., Richter, D. B., Steffen, W., Syvitski, J., Vidas, D., Wagreich, M., Williams, M., Zhisheng, A., Grinevald, J., Odada, E., Oreskes, N., Wolfe A.P. (2016). The Anthropocene is functionally and stratigraphically distinct from the Holocene. *Science*, 351(6269), aad2622.

493 **Figure captions**

494 **Figure 1.** Geographical locations where sediment cores were collected.

495 **Figure 2.** *Plum* and CF age-depth models for TEHUA-II. Plum 95% credible intervals
496 and mean are shown as red dashed lines, and dark shadow show some iterative
497 chronologies obtained by the MCMC. The CF age-depth model is shown in blue,
498 using linear interpolation between neighbouring data points used to construct the
499 model. Bottom boxes show depths where samples were analyzed. The orange box
500 shows the ^{137}Cs 1963 time marker.

501 **Figure 3.** *Plum* and CF age-depth models for core EU-III. For explanation of symbols
502 and colours, see Fig. 2.

503 **Figure 4.** *Plum* and CF age-depth models for SAMO14-2. For explanation of
504 symbols and colours, see Fig. 2.

505 **Figure 5.** *Plum* and CF age-depth models for core IXW-500. For explanation of
506 symbols and colours, see Fig. 2. In the “Supported ^{210}Pb” upper panel, black dots
507 represent *Plum* simulations, blue dots are the mean of the simulated values and red
508 dots are the ^{226}Ra measurements

509

510 **Table 1.** Sampling information for sediment cores from Mexican marine and
511 lacustrine areas.

Core ID	Coordinates	Sampling date and depth (m)	Length (cm)	Sediment characteristics	Corer type and internal diameter (cm)
IXW-500[a]	19°26.649′ N	06/08/2015	25	Marine muddy	Multicorer
	93°53.323′ W	1010		>94% silt + clay	9.5
TEHUA-II[b]	15° 59.987’ N	15/10/2004	18	Marine sandy	Reineck
	94° 48.469’ W	67		>75% sand	7
EU-III[c]	23°09.322’N	05/05/2012	50	Coastal hypersaline	Push core
	106°19.672’W	0		>60% silt	10
SAMO14-2[d]	21°22.187’ N	28/04/2019	78	Lacustrine	Uwitec™
	104°34.335’W	48		>80% silt	8.6

512 [a]Ruiz-Fernández et al., 2019a; [b]Ruiz-Fernández et al., 2009b, [c]Ruiz-Fernandez et
513 al., 2016; [d]Ruiz-Fernandez et al., 2019b.
514

Comparing classical and Bayesian ^{210}Pb dating models in human-impacted aquatic environments

*Marco A. Aquino-López, Ana Carolina Ruiz-Fernández, Maarten Blaauw, Joan-Albert Sanchez-Cabeza**

Answers to reviewers

Dear Editor,

We thank you for your support to revise our manuscript, and thank the reviewers for their efforts in reviewing this manuscript.

We have addressed each issue mentioned by the reviewers, provide an answer in this document, and the manuscript changes are shown in track mode. We have also used the opportunity to make some minor editorial changes.

We sincerely hope that the manuscript is now acceptable for publication.

Best regards,

Prof. J.A. Sanchez-Cabeza
UNAM

Reviewer #1

As the time interval covered by the Pb-210 lasts only 100 years, any extrapolation beyond this range is quite speculative. Despite the warnings in the present manuscript, it is quite dangerous to propose, as valid ages, extrapolations down to 300-400 years. Even applying C-14 ages together, it will be difficult to validate this extrapolation, because of the marine reservoir effect. Therefore, I would like to propose to restrict ages not older than 150 years.

This point was addressed in the original paper (Aquino-López et al. 2018). In the section named Chronology Limit, the use of a dynamic age limit was discussed, which takes into consideration not only a single value like the one presented by Appleby (1998), or alternative values such as 100 or 150 yr. Aquino-López et al. (2018) presented a series of simulated data where we know the true age values, and this allows us to observe the accuracy of the model. These simulations show that the model does not loose accuracy even in older ages, even though error estimates become larger. Users which are uncomfortable with large uncertainties can decide to discard portions of the age-depth model, but we feel this should be left to user discretion and to the levels of uncertainty relevant to each study.

In fact, the authors of this manuscript are in debate about the validity of extensions of several decades up to centuries. Further research based on simulations is planned to properly test this important issue. However, this is outside of the scope of the current manuscript, and we have clarified this in the revised version.

In order to clarify the issue and focus the reader interest, we have summarized sub-section *5.4 Plum extended chronologies* and the second last paragraph of the discussion section as:

> 5.4. Plum extended chronologies
> *As shown, Plum is able to obtain longer chronologies. In some cases, the extension is a result of fewer samples being used exclusively to infer supported ^{210}Pb and/or the use of the final sample with $^{210}Pb_{ex}$ not being discarded (which is common practice when using the CF model). These extensions provide an accurate chronology with an uncertainty similar to the rest of the chronology. In other cases, like IXW-500, it is the result of using ^{226}Ra concentrations combined with a sediment with ^{210}Pb in equilibrium. Plum provides a much larger extension in these chronologies, but this should be taken with extra caution, since at depths below where $^{210}Pb_{ex}$ is available, age uncertainties become considerably higher and precision decreases. These extensions are a linear simplification, which uses information from both the data and the prior distributions for the accumulation rate and variability. Under simulation, we have observed that these extensions become more inaccurate with depth, but the credible intervals (larger than in the rest of the chronology) are able to capture the true age. These extensions are rather qualitative and should not be used to obtain conclusions on sedimentary processes and records. Because simulations are not within the scope of the present study, these are left for future research.*

Also, we have included a paragraph in the Conclusions section:

> *Plum' older ages, obtained by the usability of more data, appears to be in disagreement with previous chronology limits (Appleby, 1998). This point was previously addressed by Aquino-López el at. (2018), as by using simulations it was shown that these older ages remained accurate when the core is fully sampled. These older ages are also accompanied by a more realistic uncertainty (much larger credible intervals), and should be handled with caution, even more when the core was not fully sampled. Users and/or studies which require less uncertainty should consider discarding these older ages or providing the model with other time markers, which will improve the levels of uncertainty and help the model provide a more precise chronology.*

Note that not all C-14 dates in the case studies were from marine sites.

Reviewer #2

This publication is an example of the use of the new Bayesian PLUM model to date sedimentary boreholes using lead-210 measurements. It perfectly illustrates the interest of this model compared to more classical models (here the CRS model).

I would have liked an example of the Bayesian approach also using artificial radionuclides to see the complete interest of the model as well as to understand the integration of additional proxy in PLUM. In the end, is the approach completely independent of the model user or does the user tune the model in the same way as Bacon. In this case, the most important thing is that the users of the lead-210 data clearly explain their assumptions, basic data etc. (Mustaphi et al. 2019). This work deserves prompt publication.

Many thanks to the reviewer for the positive comments. We decided to not incorporate data points of artificial radionuclides into the Plum age-models, so as to provide fair comparisons with the CRS model which uses such time markers as validation only. The manuscript states: "Plum also can use information from time-markers such as the human-made peak in ^{137}Cs to refine the age-depth model, but this was ignored as we wanted to observe only the behaviour of the ^{210}Pb data on their own." The incorporation of other dating techniques is left to future studies where we will discuss the effect and benefits this additional information has on the resulting chronology.

As for the comment on 'tuning': Plum, like Bacon, is a Bayesian approach that uses prior distributions to reconstruct the age-depth relationship. Although the default settings have been set to allow for a wide variety of sites to be age-modelled, for some cores these values need to be modified. We believe that no approach can produce entirely automated age-models without any user input. If so desired however, the approach could be modified by replacing the *Bacon* component by, say, *BChron* which has fewer user-provided settings.

Minor comments:

l. 83 explain BACON acronym

Bacon is not an acronym, but we have now clarified the model:

> *… (based on Bacon, a Bayesian piece-wise linear model constrained by prior information on accumulation rate and variability; Blaauw and Christen 2011).*

l.316: user's input: please rephrase.

Rephrased to *"... is not a value to be provided by the user but..."*


Graphical Abstract

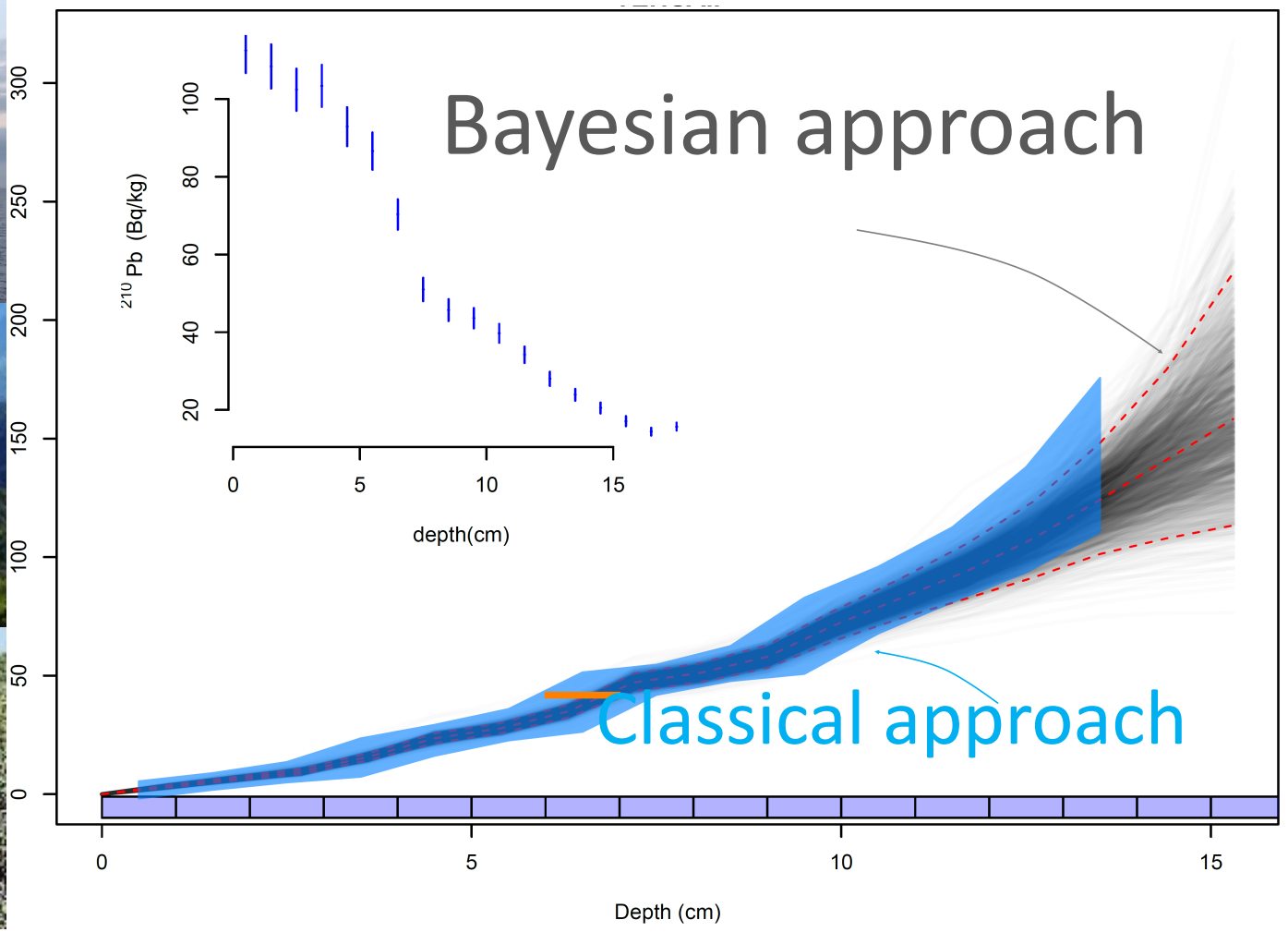
Bayesian approach
Classical approach
^{210}Pb (Bq/kg)
depth(cm)
Depth (cm)
0
50
100
150
200
250
300
20
40
60
80
100
0
5
10
15

Comparing classical and Bayesian ^{210}Pb dating models in human-impacted aquatic environments

Marco A. Aquino-López[1], Ana Carolina Ruiz-Fernández[2], Maarten Blaauw[3], Joan-Albert Sanchez-Cabeza[2]*

[1] *Maynooth University, Arts and Humanities Institute, Maynooth, Co. Kildare, Ireland.*

[2] *Unidad Académica Mazatlán, Instituto de Ciencias del Mar y Limnología, Universidad Nacional Autónoma de México, 82040 Mazatlán, México*

[3] *School of Natural and Built Environment, Queen's University Belfast, Belfast, UK.*

* Corresponding author: jasanchez@cmarl.unam.mx

Abstract

Chronologies are an essential tool to place natural archives of environmental changes on a calendar scale. Because of this, studies that compare and assess the accuracy and precision of available dating models are essential. ^{210}Pb is a radioactive isotope which is used to date recent sediments (<150 yr). Here we contrast the chronologies resulting from two different ^{210}Pb dating models: the Constant Flux model (also known as the Constant Rate of Supply model) and the recently developed Bayesian *Plum* model. This comparison was implemented by using four sediment cores from contrasting environmental settings, and showed several benefits of using a Bayesian approach. This allows to infer variables, such as the supported levels of ^{210}Pb, crucial to the chronology and commonly estimated through either samples where an asymptotic behaviour is observed or through ^{226}Ra measurements, which themselves contain some level of uncertainty. Another step of traditional methods is the selection of the equilibrium depth in order to calculate total inventories, which carries strong consequences for the resulting age depth model. *Plum*, on the other hand, infers the ^{210}Pb flux, which eliminates the need to select an equilibrium depth and allows for dating cores with incomplete inventory. When traditional methods address cores with missing inventory, ^{137}Cs time markers are commonly used to correct the chronology, but *Plum* can use these time markers to improve the chronology and to reduce the uncertainty. These aspects show that the Bayesian approach results in more robust and objective chronologies, and thus in better reconstructions of environmental change over the past centuries.

Keywords: ^{210}Pb sediment dating, Bayesian Statistics, Uncertainty, Marine, Coast, Lake.

1. Introduction

Historical records of global change provide essential information to identify the main stressors affecting ecosystems. Such environmental information can feed models of potential impact scenarios and guide the development of appropriate mitigation strategies. However, because long-term instrumental records are still scarce, natural archives such as sediment cores from aquatic ecosystems that accumulate continuously, have become one of the most relevant resources of retrospective information to establish trends of environmental changes on time-scales from years to millennia or more. This information, which includes rates of change, ages of events and timing differences between records, should be based on reliable chronologies.

^{210}Pb is the most widely used radionuclide to date sediment records within the past 110-150 years, a period that includes the Anthropocene, with huge global changes associated with the need to provide food and energy resources to a rapidly growing human population (Waters et al., 2016). ^{210}Pb ($t_{½}$=22.23 years) belongs to the ^{238}U natural decay series, and its abundance in sediments ($^{210}Pb_{tot}$) results from the mixture of (a) supported ^{210}Pb ($^{210}Pb_{sup}$) produced *in situ* through the decay of ^{226}Ra in the lithosphere, and (b) excess ^{210}Pb ($^{210}Pb_{ex}$) produced after ^{222}Rn decay and transferred to sediments through dry and wet deposition, water column scavenging and runoff. Because $^{210}Pb_{ex}$ is deposited at the sediment's surface and decays over time, its activity decreases with increasing sediment depth in cores from undisturbed sediment deposits, enabling the establishment of chronologies (Appleby and Oldfield, 1992).

61 The Constant Flux (CF) model, also known as the Constant Rate of Supply
62 (CRS), (Robbins, 1978; Appleby, 1978) is a robust and widely used ^{210}Pb dating
63 model. It is based on the fundamental equation that establishes that $^{210}Pb_{ex}$ activities
64 depend on the $^{210}Pb_{ex}$ flux to the sediment surface and the sediment mass loading
65 (Krishnaswamy et al., 1971; Sanchez-Cabeza and Ruiz-Fernández, 2012). The
66 main hypothesis behind the CF model is that the $^{210}Pb_{ex}$ flux is constant, and this
67 can be used to infer estimates of temporal variations of sediment accumulation rates
68 (SAR, cm $year^{-1}$) and mass accumulation rates (MAR, g cm^{-2} $year^{-1}$). Age
69 calculations are based on the total inventory of $^{210}Pb_{ex}$ (i.e. the accumulated deposit
70 per unit area), which requires estimates of $^{210}Pb_{ex}$ data for each core section until
71 reaching the equilibrium depth (where $^{210}Pb_{tot}$ and $^{210}Pb_{sup}$ activities become
72 indistinguishable). Therefore, missing $^{210}Pb_{ex}$ data should be estimated by
73 interpolation or, in the case of cores not reaching equilibrium, missing inventory
74 extrapolated (Appleby, 2002). These restrictive requirements might cause problems
75 in sub-optimal cores (e.g., those with incomplete $^{210}Pb_{ex}$ inventory, poorly defined
76 ^{210}Pb equilibrium depth, or varying $^{210}Pb_{sup}$). Therefore, some CF-derived age-
77 models may not provide reliable chronologies, especially given the extensive global
78 land use changes that have taken place over the past century.
79 Recently, Aquino-López et al. (2018) developed a new model for ^{210}Pb dating
80 called *Plum*, which is also based on the fundamental equation and the CF
81 hypothesis. *Plum* is a Bayesian forward model that simultaneously integrates two
82 different processes: (1) the behaviour of the ^{210}Pb flux and the variation of $^{210}Pb_{sup}$
83 with depth, and (2) an age-depth function (based on *Bacon, a Bayesian piece-wise*
84 *linear model constrained by prior information on accumulation rate and variability*;

85 Blaauw and Christen 2011). These processes are parameterized, which allows the
86 use of a Bayesian approach. With the help of millions of Monte Carlo Markov Chain
87 (MCMC) iterations, a posterior sample can be obtained. This posterior sample
88 combines *a priori* information of sediment accumulation rates, $^{210}Pb_{ex}$ flux (typically
89 observed in a given sampling site type) and data ($^{210}Pb_{tot}$ and ^{226}Ra laboratory
90 measurements, and potentially additional information from other radioactive isotopes
91 such as ^{137}Cs and ^{14}C). Within any of the iterations, *Plum* chooses values for both
92 the age-depth function, which assigns ages to any depth, and the ^{210}Pb flux and
93 $^{210}Pb_{sup}$. With these parameters and the given ^{210}Pb's known $t_{½}$, values for $^{210}Pb_{tot}$
94 can be calculated and compared to the measurements at any depth. *Plum* only
95 requires experimental data on sediment density, $^{210}Pb_{tot}$ and ^{226}Ra activities (or at
96 least a good approximation of $^{210}Pb_{sup}$) and the outputs include estimates of $^{210}Pb_{xs}$
97 flux, supported ^{210}Pb and sediment ages. Any of these parameters are expressed
98 as posterior distributions and 95% confidence intervals.
99 In comparison to the traditional implementation of the CF model, which is a
100 reverse and deterministic model (e.g. ages are directly inferred from $^{210}Pb_{tot}$ and
101 ^{226}Ra laboratory data), *Plum* is a much more flexible forward model that allows
102 coping with non-ideal ^{210}Pb depth profiles (variable compaction poorly-defined
103 equilibrium depth). In addition, it can easily handle gaps in ^{210}Pb data or multiple
104 measurements even from the same depth, and can include other types of dating
105 information (e.g. ^{14}C dates, ^{137}Cs peak and tephras).
106 In this work, we present results of a test on the efficacy and reliability of the
107 CF and *Plum* models using data of previously published ^{210}Pb-dated sediment cores
108 from contrasting environments (deep and shallow marine areas, a crater lake, and a

109 saltmarsh) where dating difficulties were encountered. Our hypothesis was that *Plum*
110 is better than CF in managing the assumptions involved with the ^{210}Pb CF model
111 and in estimating age uncertainties. The age models obtained were contrasted with
112 stratigraphic markers (e.g. ^{137}Cs, Pu isotopes) for validation.

113 **2. Study area**

114 The sediment cores were collected from four contrasting environments in Mexico, in
115 order to reconstruct the temporal trends of a range of global change indicators
116 (Figure 1). Core IXW-500 (Ruiz-Fernández et al., 2019a) was collected from a deep-
117 sea area in the southern Gulf of Mexico (Atlantic Coast) characterized by strong
118 fluvial input, natural oil seeps, intense maritime traffic and offshore oil extraction
119 activities, and was used to assess trace metal contamination.

120 Core Tehua-II (Ruiz-Fernández et al., 2009b) was sampled from a shallow
121 marine area in the Tehuantepec Gulf (Pacific Coast) characterized by high
122 productivity associated with fluvial inputs and intense upwelling, which sustains
123 relevant commercial fisheries (e.g. tuna, shrimp and shark) and experiences strong
124 shipping traffic owing to oil production and distribution activities. For this core,
125 temporal variations of sediment accumulation rates were determined in order to
126 reconstruct land use changes.

127 Core AIII (Ruiz-Fernández et al., 2016) was sampled to estimate rates of sea
128 level rise at a saltmarsh in Estero de Urías (Gulf of California, Pacific Coast) an
129 anthropized lagoon that hosts a harbour with shipping activities ranging from
130 cabotage and fishing (mainly tuna and shrimp) to passenger cruises, and which also
131 receives untreated domestic and industrial wastes.

Finally, core SAMO2014-2 (Ruiz-Fernández et al., 2019b) was collected to determine mass accumulation rates in Lake Santa Maria del Oro, a 2-km diameter and 65m deep oligomictic and mesotrophic crater lake (Cardoso-Mohedano et al., 2019). The lake is mainly used for recreational activities, and it is located within the Trans-Mexican Volcanic Belt at 65 km from the Pacific Coast.

3. Methods

The sediment cores were collected with transparent PVC tubes of different internal diameter and assisted by different types of samplers (see Table 1 for sampling details). The cores were extruded and cut into contiguous 1 cm thick sections. Samples were weighed before and after freeze-drying; sediment bulk density (g cm^{-3}) was calculated as the ratio of the total dry mass and the volume (from diameter and thickness) of each core section.

3.1. Laboratory analysis

All sediment cores were analysed in the Sediment Dating Academic Service at UNAM, following the methodology described in previous publications (Ruiz-Fernández et al., 2009, 2016, 2019a, 2019b). To summarise, $^{210}Pb_{tot}$ activities were measured using alpha spectrometry (Alpha Ensemble Ortec/Ametek) according to Ruiz-Fernández and Hillaire-Marcel (2009). $^{210}Pb_{sup}$ activities were estimated using gamma spectrometry measurements of ^{226}Ra activities (through its daughter radionuclide ^{214}Pb, 352 keV) using a low-background Ortec HPGe well-detector (Ruiz-Fernández et al., 2014). $^{210}Pb_{xs}$ activities were determined using the difference between $^{210}Pb_{tot}$ and $^{210}Pb_{sup}$ activities. To validate the ^{210}Pb-derived chronologies, the activity profiles of ^{137}Cs against depth were determined by gamma-ray spectrometry (662 keV) in all cores, and plutonium isotopes were determined by i)

156 alpha-particle spectrometry for core SAMO14-2 (Ruiz-Fernández et al., 2019b), ii)
157 low-energy accelerator mass spectrometry for core EUIII (in Centro Nacional de
158 Aceleradores, Spain; Ruiz-Fernández et al., 2016) and iii) mass spectrometry in
159 Spiez Laboratory (Switzerland) for core IXW-500.

160 *3.2. ^{210}Pb-derived chronologies*

161 In the original papers, chronologies, mass and sediment accumulation rates were
162 estimated with the constant flux (CF) model (Appleby and Oldfield, 1978; Robbins,
163 1978; Sanchez-Cabeza and Ruiz-Fernández, 2012). Dating uncertainties in core
164 Tehua-II were calculated using quadratic propagation uncertainty, whereas in the
165 other cores they were estimated by Monte Carlo simulation with 10^5 simulations
166 (Sanchez-Cabeza et al., 2014).

167 The *Plum* age-depth models were obtained using the default settings. These
168 settings dictate the prior distributions used for the supported ^{210}Pb, ^{210}Pb flux, and
169 sedimentation rate and its variability (used within each *Bacon* section), as well as
170 the thickness of *Bacon* sections. By default, *Plum* uses 1-cm thick *Bacon* sections
171 (whereas *Bacon*'s default is 5, which is probably too restrictive to model
172 sedimentation close to the surface). The default prior distribution for the supported
173 ^{210}Pb parameters is a gamma distribution with a mean of 15 Bq kg^{-1} and a shape
174 parameter of 2. For core IXW500, *Plum* used the ^{226}Ra measurements to obtain
175 estimates for supported ^{210}Pb at multiple depths, whereas for the other cores
176 supported ^{210}Pb was assumed to be constant throughout each core. For the ^{210}Pb
177 flux, *Plum* uses a gamma distribution with a mean of 50 Bq m^{-2} yr^{-1} and a shape
178 parameter of 2. *Plum* also uses an upper age limit, for which it uses a parameter set
179 to A_l=0.1 by default, which is defined as the remaining unmeasured $^{210}Pb_{ex}$. This

180 variable allows for faster convergence of the MCMC, and limits the chronology
181 according to the inferred $^{210}Pb_{ex}$ flux. *Plum* also can use information from time-
182 markers such as the human-made peak in ^{137}Cs to refine the age-depth model, but
183 this was ignored as we wanted to observe only the behaviour of the ^{210}Pb data on
184 their own.

185 **4. Results**

186 Figures 2, 3, 4 and 5 show the comparisons between the ^{210}Pb-derived chronologies
187 using the CF and *Plum* dating models.

188 *4.1. TEHUA-II*

189 In the case of TEHUA-II (Figure 2), both models agreed well with each other
190 throughout the chronologies. The CF confidence intervals overlapped *Plum*'s
191 credible intervals, i.e. *Plum* provided narrower intervals. In this case, *Plum* was able
192 to extend the chronology by up to two decades, because fewer measurements were
193 discarded in order to infer the supported ^{210}Pb. Both models agreed quite well with
194 the 1963 time-marker.

195 *4.2. EU-III*

196 Figure 3 shows the comparison between the *CF* and *Plum* age-models of core EU-
197 III. In this case, the chronologies agreed well with each other, providing similar age
198 estimates and similar credible and confidence intervals. Again, *Plum* was able to
199 extend the chronology for several decades as several more data points are used to
200 infer the chronology: CF inferred a chronology up to a depth of 27.5 cm, whereas
201 *Plum* reached a depth of 39 cm. Regarding the 1963 time marker, *Plum* seems to
202 agree better as the CF model provided younger ages and its uncertainty was
203 insufficient to enclose the time marker.

204 *4.3. SAMO14-2*

205 SAMO14-2's chronology (Figure 4) showed that the age estimates are in good
206 agreement and both models enclose the time marker within its intervals. On the other
207 hand, the model's uncertainty estimates show largeed differences, with *Plum*
208 providing more conservative uncertainty estimates. Regarding the length of the
209 chronology, *Plum* was again able to extend the chronology by several decades by
210 its use of fewer measurements to infer the supported ^{210}Pb value.

211 *4.4. IXW-500*

212 In this case, the CF- and *Plum*- derived age models resulted in significant differences
213 (Fig. 5) at different core depths. In comparison with CF ages, *Plum* ages were older
214 in the segments surface – 4 cm and 8 – 12 cm, but comparable within the segments
215 5 – 8 cm and below 12 cm. *Plum* provided a more conservative age estimate, with
216 larger and more credible intervals than the CF model. In this particular case, The
217 *Plum*-derived age model comprised almost twice the CF age period (age estimate
218 of 160 years at 15 cm depth and 308 years at 29 cm depth). This was caused by CF
219 having to discard the 5 bottom measurements, whereas *Plum* was able to extract
220 information from them.

221 The considerable differences between the models could be caused by the
222 peculiar ^{226}Ra profile of this core (shown as blue dots in the supported ^{210}Pb panel
223 in Figure 4). The largest difference between the age models was observed at mid-
224 depth, where a minimum $^{210}Pb_{ex}$ in activity occurs, caused by large ^{226}Ra activity.
225 This also resulted in both models presenting a change in behaviour at this depth,
226 with a larger accumulation rate at depths lower than 9 cm. In this case, refining the
227 chronology using more information (e.g. ^{137}Cs) could be of help, as *Plum* can include

these time markers to the likelihood function in order to obtain an integrated chronology.

It is important to note that both total ^{210}Pb and ^{226}Ra at the five deepest samples were very similar, i.e. equilibrium was reached. In this case, *Plum* uses the information provided by the rest of the core and the prior distribution to provide an informed extrapolation.

5. Discussion

5.1. Tehua-II and EU-III

As all sections of these cores were measured down to equilibrium, as expected both models provided similar results. In the case of TEHUA-II, *Plum* provided narrower credible intervals, which are a result of the use of the *Bacon* age-depth function, instead of the decay equation used by the CF model. On the other hand, the age-models for EU-III agreed well and reconstructed similar uncertainty intervals. *Plum* was able to extend the chronology by a couple of decades in the case of TEHUAII and by more than 100 yr in the case of EU-III. This is a result of *Plum*'s integration of supported ^{210}Pb in the inference process, removing the need to discard the lowermost few measurements.

5.2. SAMO14-2

SAMO14-2 presents an interesting case as relatively few data points were available for the inference. Both models presented overlapping results. In this case, *Plum* provided wider intervals as a result of the low number of samples measured for this core. The CF model provided very precise age estimates, apparently a positive outcome, but considering that less than 25% of the core sections were measured (10 measurements of 1 cm sections were used to infer the chronology to a depth of

252 41 cm), the more conservative intervals provided by *Plum* are more coherent. This
253 is an important consequence of the interpolations used to estimate the $^{210}Pb_{ex}$
254 inventories, which do not consider the error caused by the absence of
255 measurements. Interestingly, something similar appears to happen in simulated and
256 real-world ^{14}C-dated cores modelled using classical and Bayesian age-models
257 (Blaauw et al. 2018): whereas Bayesian age-models become more precise with
258 increasing dating densities (they 'learn'), classical age-models such as linear
259 interpolation do not.

260 *5.3. IXW-500*

261 This core presented significant differences between each model. *Plum* inferred lower
262 levels of supported ^{210}Pb at 8 – 10 cm depths in comparison to the measured ^{226}Ra
263 (see Figure 5). It is at these depths where both models show their largest
264 discrepancies. In this case, more measurements around the spike of ^{226}Ra could
265 help *Plum* to model these unusual spikes. Also, *Plum* can use other time markers
266 such as ^{137}Cs to refine the chronology.

267 *5.4. Plum extended chronologies*

268 As shown, *Plum* is able to obtain longer chronologies. In some cases, the extension
269 is a result of fewer samples being used exclusively to infer supported ^{210}Pb and/or
270 the use of the final sample with $^{210}Pb_{ex}$ not being discarded (which is common
271 practice when using the CF model). These extensions provide an accurate
272 chronology with an uncertainty similar to the rest of the chronology. In other cases,
273 like IXW-500, it is the result of using ^{226}Ra concentrations combined with a sediment
274 with ^{210}Pb in equilibrium. *Plum* provides a much larger extension in these
275 chronologies, but this should be taken with extra caution, since at depths below

where $^{210}Pb_{ex}$ is available, age uncertainties become considerably higher and precision decreases. These extensions are a linear simplification, which uses information from both the data and the prior distributions for the accumulation rate and variability. Under simulation, we have observed that these extensions become more inaccurate with depth, but the credible intervals (larger than in the rest of the chronology) are able to capture the true age. These extensions are rather qualitative and should not be used to obtain conclusions on sedimentary processes and records. Because simulations are not within the scope of the present study, these are left for future research.

5.5. CF rapid accumulation

The CF model was constructed using the decay equation as its basis, which resulted in a logarithmic age-depth function; $t(x) = \lambda^{-1} log\left(\frac{A(0)}{A(x)}\right)$. This age-depth function works well in the most recent part of the sediment, but as the remaining activity $A(x)$ gets close to 0, the age function rapidly tends to infinity, resulting in an artificial increase of accumulation rates. This increase is not caused by natural sources but it is a result of the mathematical structure of the model and should not be included in interpretations. On the other hand, because *Plum* uses an independent age-depth function, it does not show this artificial increase in accumulation, providing a more realistic age-depth function at deeper parts of the sediment.

5.6. Overall considerations

When CF model users are confronted with a new core, a number of decisions must be made based on the available information. Because of resource constraints, typically not all core sections are measured and interpolation techniques are needed,

299 which may induce an experimental error. By design, *Plum* does not need any kind
300 of interpolation and solely relies on the existing data. While both the CF model and
301 *Plum* should produce better age-models with more data (i.e. more information), *Plum*
302 results are undoubtedly more reliable when some data are missing.

303 The reliability of measurement can also be sometimes an issue. For example,
304 the CF radiochronologist might decide that a measurement is an outlier, or that
305 concentrations close or below 0 Bq kg^{-1} are zero. In the case of *Plum*, this is not an
306 issue, as the system will choose, based on Bayesian statistics, which is the best set
307 of activities and, in some cases, disregard an outlier or ignore low (or negative)
308 concentrations, without human intervention.

309 One of the critical decisions that must be taken when using the CF model is
310 the selection of the equilibrium depth of the core, i.e., the depth where the $^{210}Pb_{ex}$
311 reaches zero and from where the total $^{210}Pb_{ex}$ inventory can be calculated. The
312 equilibrium depth mainly depends on the unambiguous knowledge of the $^{210}Pb_{sup}$
313 value. This is often difficult to ascertain owing to i) large relative uncertainties of
314 $^{210}Pb_{ex}$, when calculated by subtraction of ^{210}Pb and ^{226}Ra (or an estimated $^{210}Pb_{sup}$),
315 which can be very similar at the core bottom, and ii) changes in sediment
316 composition which can produce variations of $^{210}Pb_{sup}$ activities along a core (e.g.
317 Carnero-Bravo et al. 2016), which will affect the total $^{210}Pb_{xs}$ inventory and thus the
318 core age, as higher inventories will cause younger ages and vice versa. Therefore,
319 depending on the core's ^{210}Pb activity profile, small variations of specific activities
320 could produce age variations amounting to decades. A relevant feature of *Plum* is
321 that $^{210}Pb_{sup}$ is not a a value to be provided by the user but a parameter to be inferred.
322 *Plum* uses data to infer $^{210}Pb_{sup}$, which can be ^{226}Ra measurements or ^{210}Pb which

323 reached equilibrium. If only ^{210}Pb is available, *Plum* runs a pre-analysis based on a
324 linear regression, where the segment which provides the largest p-value (and thus
325 lower variability) is suggested to be used exclusively to infer $^{210}Pb_{sup}$. Because the
326 p-value is affected by sample size, this pre-analysis should be confirmed by the user,
327 but it has provided reasonable results in several simulations and real cores. This
328 reduces considerably the calculation efforts and decisions of the user, and
329 maximizes the confidence in the $^{210}Pb_{sup}$ value.

330 Sometimes the ^{210}Pb profile is incomplete, i.e. ^{210}Pb does not reach
331 equilibrium. In this case, CF users need to estimate the missing inventory from either
332 a bottom constant accumulation rate, or by using a reference date (e.g. the ^{137}Cs
333 maximum). In the case of *Plum* this is not needed, as even in these cases *Plum* will
334 estimate the total $^{210}Pb_{ex}$ flux by Bayesian statistics.

335 In overall, these and other decisions may cause different scientists, or even
336 the same scientist at different moments, to produce different chronologies with the
337 same data set and using the same model. As *Plum* uses existing information, age
338 models should be identical (as long as the prior parameters are the same) and the
339 user-based bias should largely reduced. In this sense, *Plum* is clearly more objective
340 and we suggest that it should be widely used by ^{210}Pb radiochronologists.

341 In this comparison study, only ^{210}Pb measurements were used to produce
342 chronologies. However, for core IXW-500 additional nuclides were measured,
343 including ^{137}Cs, which has known historical peaks caused by radioactive releases
344 into the atmosphere. Such peaks are regularly used to validate or adjust ^{210}Pb-based
345 chronologies. *Plum* can integrate such information, as well as ^{14}C and other dates,
346 into the ^{210}Pb chronology.

6. Conclusions

The application of the CF ^{210}Pb sediment dating model requires from the radiochronologist several inputs, such as the equilibrium depth and data interpolation when not all sections are measured, a rather common case. However, with the Bayesian approach used by *Plum* this is no longer needed, thus making the dating process less subjective and more reproducible.

The comparison of both approaches show that *Plum* provides similar results to the classical CF model, with the added benefits of providing more precise uncertainty estimates when sampling density is high (like in the case of TEHUA-II and EU-III), and providing more realistic uncertainty estimates where few samples are available (SAMO14-2). Also, *Plum* is not affected by artificial increases of sedimentation in the deepest part of the sediment, unlike the CF model where the logarithmic age-function tends to infinity as background is reached. This allows the user to interpret dates deeper in the core without being affected by artificial increases in the sedimentation.

Plum' older ages, obtained by the usability of more data, appears to be in disagreement with previous chronology limits (Appleby, 1998). This point was previously addressed by Aquino-López el at. (2018), as by using simulations it was shown that these older ages remained accurate when the core is fully sampled. These older ages are also accompanied by a more realistic uncertainty (much larger credible intervals), and should be handled with caution, even more when the core is not fully sampled. Users and/or studies which require less uncertainty should consider discarding these older ages or providing the model with other time markers,

370 which will improve the levels of uncertainty and help the model provide a more
371 precise chronology.

372 The ability of adding extra information such as ^{137}Cs, radiocarbon dates
373 and/or tephra dates can be used for both validating the chronology or improving it.
374 Because *Plum* uses raw ^{210}Pb to create the chronology, multiple isotope
375 chronologies are possible without having to pre-model the ^{210}Pb dates. This quality
376 should not be underestimated, as the effects of the bias in the deepest part of the
377 sediment presented by the CF model have not yet been studied. Because of all these
378 considerations, we believe that *Plum* has the potential of providing more robust and
379 objective ^{210}Pb chronologies.

380 **Acknowledgements**

381 The authors acknowledge partial financial support from a Royal Society-Newton
382 Mobility Grant (Dating the decadal-scale dynamics of ENSO and pollution trends
383 from crater lake sediments in Nayarit, western tropical Mexico), CONACYT (PDCPN
384 2015-01/473, CONACYT-CNR C0013-2016-05-277942, SEMARNAT-2016-01-
385 278634), UNAM (PAPIIT IN110518 and IN104718; LANCAD-UNAM-DGTIC-273).
386 Part of this work was funded by a CONACYT postgraduate scholarship 411036 to
387 Marco A. Aquino-López at Queen's University Belfast. Authors are grateful to the
388 technical support received by L.H. Pérez-Bernal, León Felipe Álvarez, H. Bojórquez-
389 Leyva, S. Rendón-Rodríguez, G. Ramírez Reséndiz and C. Suárez-Gutiérrez.

390 **Data Availability**

391 Sediment data are available as supplementary material.

392 **Supplementary material**

393 - Data used for ^{210}Pb dating with *Plum*.

394 **References**

395 Appleby, P. G., Oldfield, F. (1978). The calculation of lead-210 dates assuming a
396 constant rate of supply of unsupported ^{210}Pb to the sediment. Catena, 5(1), 1-
397 8.

398 Appleby, P. G., Oldfield, F. (1992). Application of lead-210 to sedimentation studies.
399 Uranium-Series Disequilibrium: Applications to Earth, Marine, and
400 Environmental Sciences, 2nd edition. Oxford: Clarendon, 731-778.

401 Appleby, P. G. (1998). Dating recent sediments by 210Pb: Problems and solutions.
402 Proc. 2nd NKS/EKO-1 Seminar, Helsinki, 2-4 April 1997, STUK, Helsinki,
403 pages 7–24.

404 Appleby, P. G. (2002). Chronostratigraphic techniques in recent sediments. In
405 Tracking environmental change using lake sediments (pp. 171-203). Springer,
406 Dordrecht.

407 Aquino-López, M. A., Blaauw, M., Christen, J. A., Sanderson, N. K. (2018). Bayesian
408 analysis of ^{210}Pb dating. *Journal of Agricultural, Biological and Environmental*
409 *Statistics*, 23(3), 317-333.

410 Blaauw, M. Christen, J. A. (2011). Flexible paleoclimate age-depth models using an
411 autoregressive gamma process. *Bayesian Analysis*, 6(3), 457-474.

412 Blaauw, M., Christen, J.A., Bennett, K.D., Reimer, P.J., 2018. Double the dates and
413 go for Bayes – impacts of model choice, dating density and quality on
414 chronologies. *Quaternary Science Reviews*, 188, 58—66

415 Cardoso-Mohedano, J. G., Sanchez-Cabeza, J. A., Ruiz-Fernández, A. C., Pérez-
416 Bernal, L. H., Lima-Rego, J., Giralt, S. (2019). Fast deep water warming of a
417 subtropical crater lake. *Science of the Total Environment*, 691, 1353-1361.

418 Carnero-Bravo, V., Sanchez-Cabeza, J. A., Ruiz-Fernández, A. C., Merino-Ibarra,
419 M., Hillaire-Marcel, C., Corcho-Alvarado, J. A., Röllin, S., Diaz-Asencio, M.,
420 Cardoso-Mohedano, J.G., & Zavala-Hidalgo, J. (2016). Sedimentary records of
421 recent sea level rise and acceleration in the Yucatan Peninsula. *Science of the*
422 *Total Environment*, 573, 1063-1069.
423 Krishnaswamy, S., Lal, D., Martin, J., Meybeck, M. (1971). Geochronology of Lake
424 Sediments. *Earth and Planetary Science Letters* 11: 407–14.
425 Robbins J. A. (1978) Geochemical and geophysical applications of radioactive lead
426 isotopes. In Biochemistry of Lead (ed. J. O. Nriagu). Elsevier, Amsterdam, pp.
427 85–393.
428 Ruiz-Fernández A.C., Hillaire-Marcel C. (2009a). ^{210}Pb-derived ages for the
429 reconstruction of terrestrial contaminant history into the Mexican Pacific coast:
430 Potential and limitations. *Marine Pollution Bulletin* 59, 134–145.
431 Ruiz-Fernández A. C., Hillaire-Marcel C., de Vernal A., Machain-Castillo M. L.,
432 Vásquez L., Ghaleb B., Aspiazu-Fabián, J.A., Páez-Osuna F. (2009b).
433 Changes of coastal sedimentation in the Gulf of Tehuantepec, South Pacific
434 Mexico, over the last 100 years from short-lived radionuclide measurements.
435 *Estuarine Coastal and Shelf Science* 82, 525–536.
436 Ruiz-Fernández, A. C., Maanan, M., Sanchez-Cabeza, J. A., Pérez-Bernal, L. H.,
437 López-Mendoza, P., Limoges, A. (2014). Chronology of recent sedimentation
438 and geochemical characteristics of sediments in Alvarado Lagoon, Veracruz
439 (southwestern gulf of Mexico). Ciencias Marinas, 40(4), 291-303.
440 Ruiz-Fernández A. C., Sanchez-Cabeza J. A., Serrato de la Peña J. L., Perez-Bernal
441 L. H., Cearreta, A., Flores-Verdugo F., M. L. Machain-Castillo, Chamizo E.,

García-Tenorio R., Queralt I., Dunbar R. B., Mucciarone D.A., Diaz-Asencio M. (2016). Accretion rates in coastal wetlands of the southeastern Gulf of California and their relationship with sea level rise. *The Holocene* 26, 7, 1126–1137.

Ruiz-Fernández A.C., Sanchez-Cabeza J.A., Pérez-Bernal L. H., Gracia-Gasca A. (2019a). Spatial and temporal distribution of heavy metal concentrations and enrichment in the Southern Gulf of Mexico. *The Science of the Total Environment 651*, Part 2, 3174-3186.

Ruiz-Fernández A.C., Sanchez-Cabeza J. A., Hernández-Rivera D.M., Pérez-Bernal L. H., Cardoso-Mohedano J. G. (2019b). Historical reconstruction of sediment accumulation rates as an indicator of global change impacts in a tropical crater lake in Mexico. *In preparation.*

Sanchez-Cabeza J.A., Ruiz-Fernández A.C. (2012). ^{210}Pb sediment radiochronology: an integrated formulation and classification of dating models. *Geochimica et Cosmochimica Acta* 82, 183–200.

Sanchez-Cabeza J. A., Ruiz-Fernández AC, Ontiveros Cuadras JF, Pérez Bernal LH, Olid C (2014). Monte Carlo uncertainty calculation of ^{210}Pb chronologies and accumulation rates of sediments and peat bogs. *Quaternary Geochronology* 23, 80–93

Waters, C. N., Zalasiewicz, J., Summerhayes, C., Barnosky, A. D., Poirier, C., Gałuszka, A., Cearreta, A., Edgeworth, M., Ellis, E.C., Ellis, M., Jeandel, C., Leinfelder, R., McNeill, J. R., Richter, D. B., Steffen, W., Syvitski, J., Vidas, D., Wagreich, M., Williams, M., Zhisheng, A., Grinevald, J., Odada, E., Oreskes,

N., Wolfe A.P. (2016). The Anthropocene is functionally and stratigraphically distinct from the Holocene. *Science*, 351(6269), aad2622.

468 **Figure captions**

469 **Figure 1.** Geographical locations where sediment cores were collected.

470 **Figure 2.** *Plum* and CF age-depth models for TEHUA-II. Plum 95% credible intervals
471 and mean are shown as red dashed lines, and dark shadow show some iterative
472 chronologies obtained by the MCMC. The CF age-depth model is shown in blue,
473 using linear interpolation between neighbouring data points used to construct the
474 model. Bottom boxes show depths where samples were analyzed. The orange box
475 shows the ^{137}Cs 1963 time marker.

476 **Figure 3.** *Plum* and CF age-depth models for core EU-III. For explanation of symbols
477 and colours, see Fig. 2.

478 **Figure 4.** *Plum* and CF age-depth models for SAMO14-2. For explanation of
479 symbols and colours, see Fig. 2.

480 **Figure 5.** *Plum* and CF age-depth models for core IXW-500. For explanation of
481 symbols and colours, see Fig. 2. In the “Supported ^{210}Pb” upper panel, black dots
482 represent *Plum* simulations, blue dots are the mean of the simulated values and red
483 dots are the ^{226}Ra measurements

484

485 **Table 1.** Sampling information for sediment cores from Mexican marine and
486 lacustrine areas.

Core ID	Coordinates	Sampling date and depth (m)	Length (cm)	Sediment characteristics	Corer type and internal diameter (cm)
IXW-500[a]	19°26.649′ N	06/08/2015	25	Marine muddy	Multicorer
	93°53.323′ W	1010		>94% silt + clay	9.5
TEHUA-II[b]	15° 59.987’ N	15/10/2004	18	Marine sandy	Reineck
	94° 48.469’ W	67		>75% sand	7
EU-III[c]	23°09.322’N	05/05/2012	50	Coastal hypersaline	Push core
	106°19.672’W	0		>60% silt	10
SAMO14-2[d]	21°22.187’ N	28/04/2019	78	Lacustrine	Uwitec™
	104°34.335’W	48		>80% silt	8.6

487 [a]Ruiz-Fernández et al., 2019a; [b]Ruiz-Fernández et al., 2009b, [c]Ruiz-Fernandez et
488 al., 2016; [d]Ruiz-Fernandez et al., 2019b.
489

Figure 1

Click here to access/download;Figure;1 map 20191025.tif

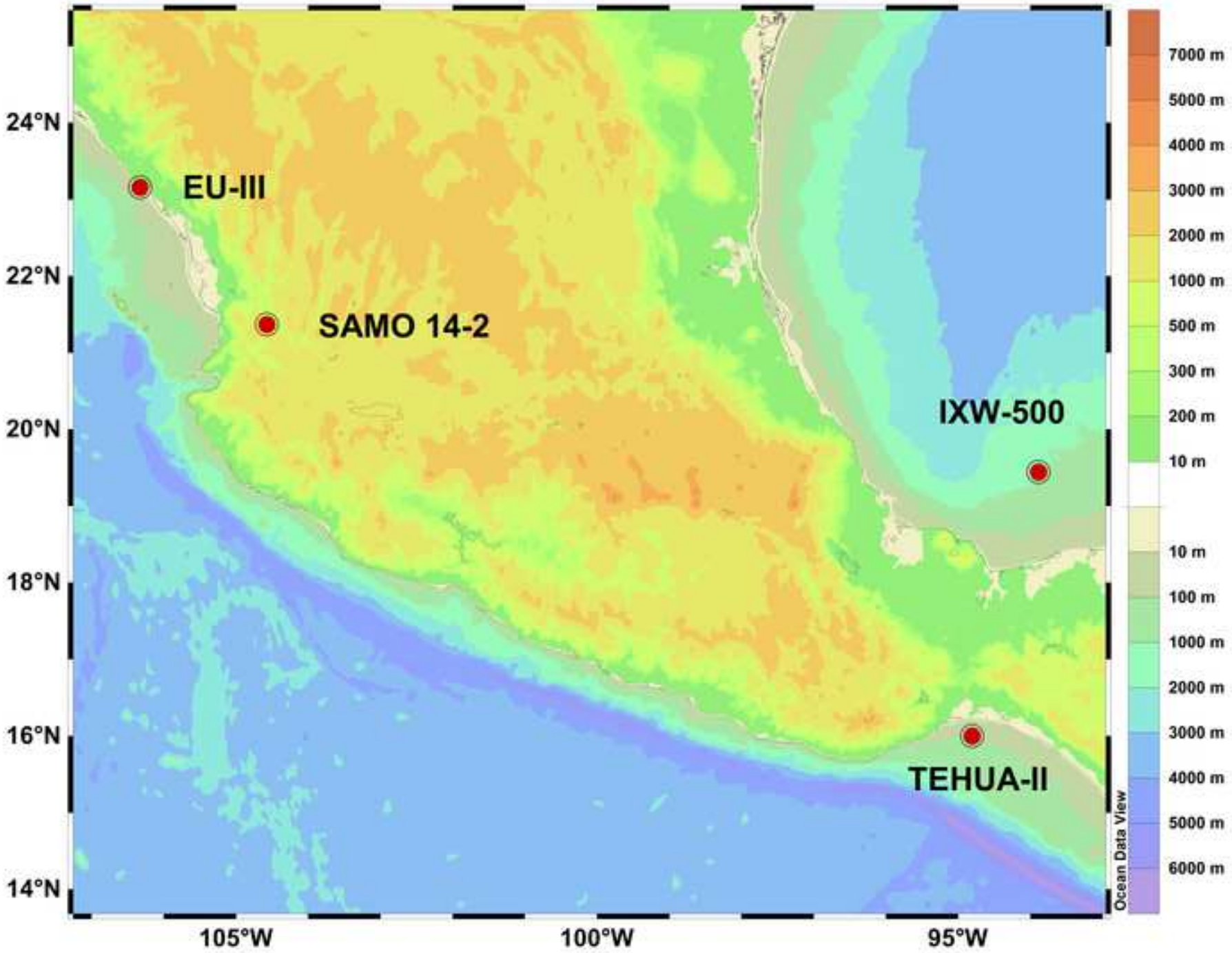

Figure 2

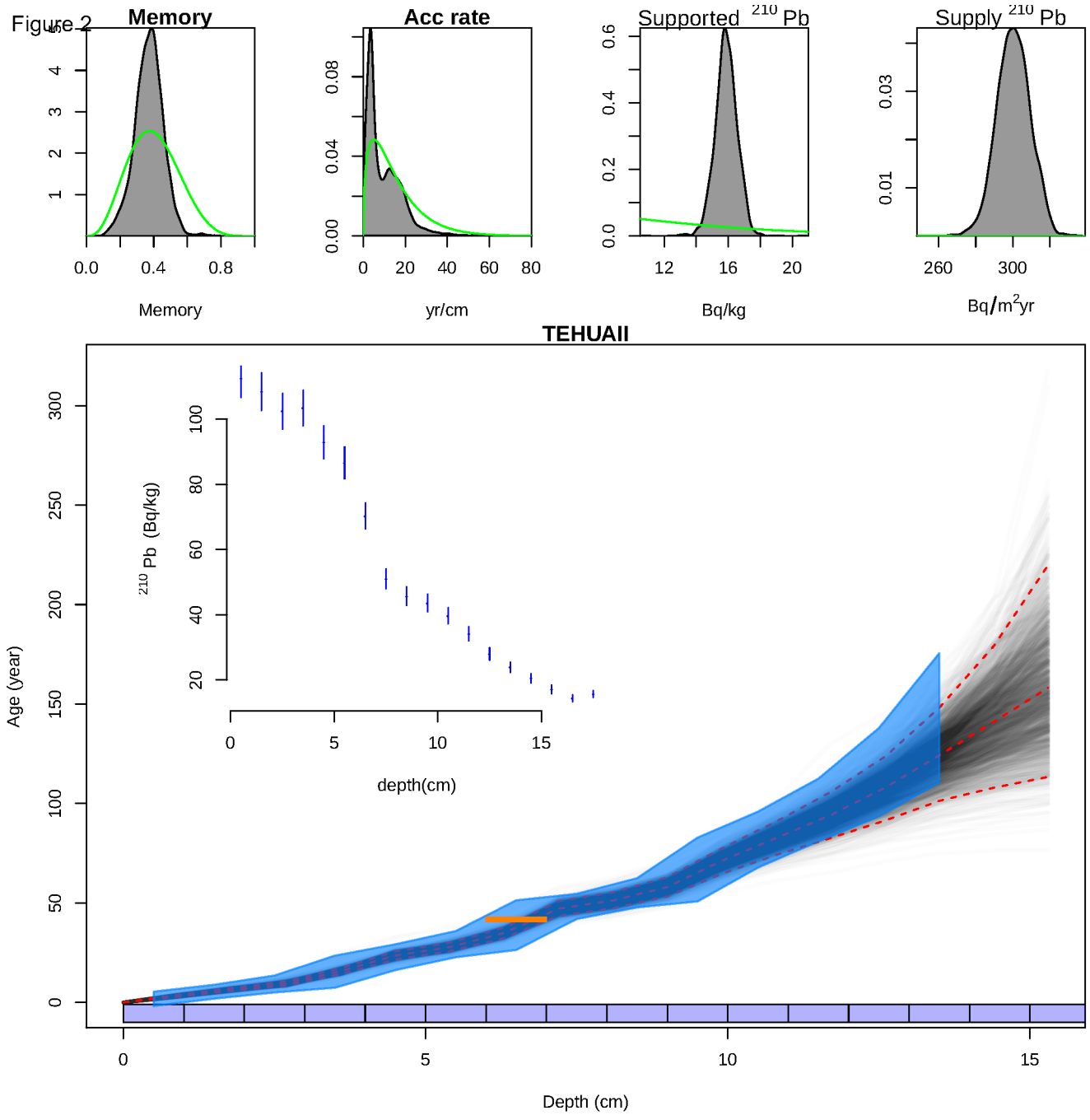
Memory
Acc rate
Supported 210 Pb
Supply 210 Pb
Memory
yr/cm
Bq/kg
Bq/m2yr
TEHUAII
210 Pb (Bq/kg)
depth(cm)
Age (year)
Depth (cm)

Figure 3

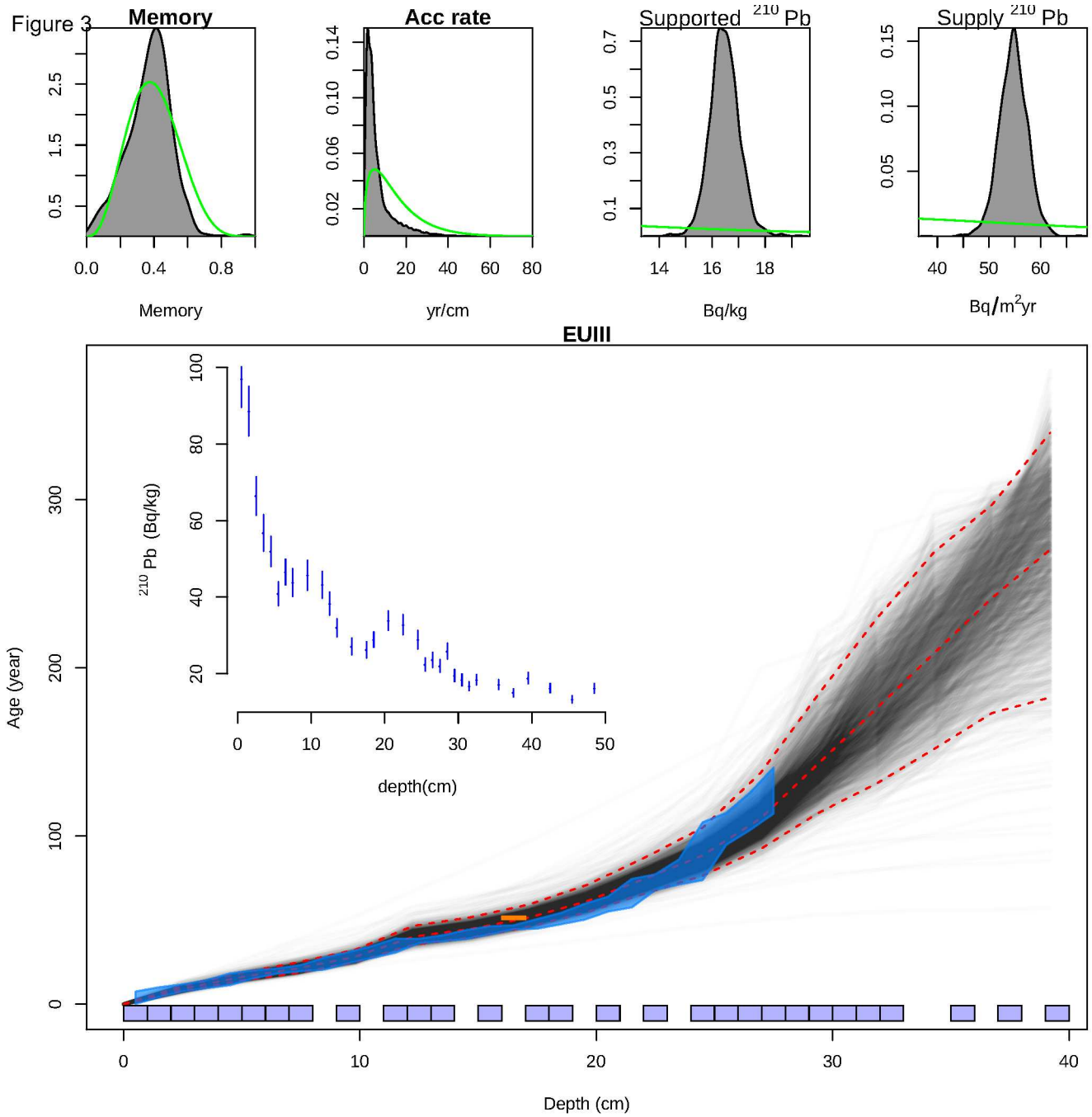
Memory
0.5
1.5
2.5
0.0
0.4
0.8
Memory
Acc rate
0.02
0.06
0.10
0.14
0
20
40
60
80
yr/cm
Supported 210 Pb
0.1
0.3
0.5
0.7
14
16
18
Bq/kg
Supply 210 Pb
0.05
0.10
0.15
40
50
60
Bq/m2yr
EUIII
Age (year)
0
100
200
300
0
10
20
30
40
Depth (cm)
210 Pb (Bq/kg)
20
40
60
80
100
0
10
20
30
40
50
depth(cm)

Figure 4

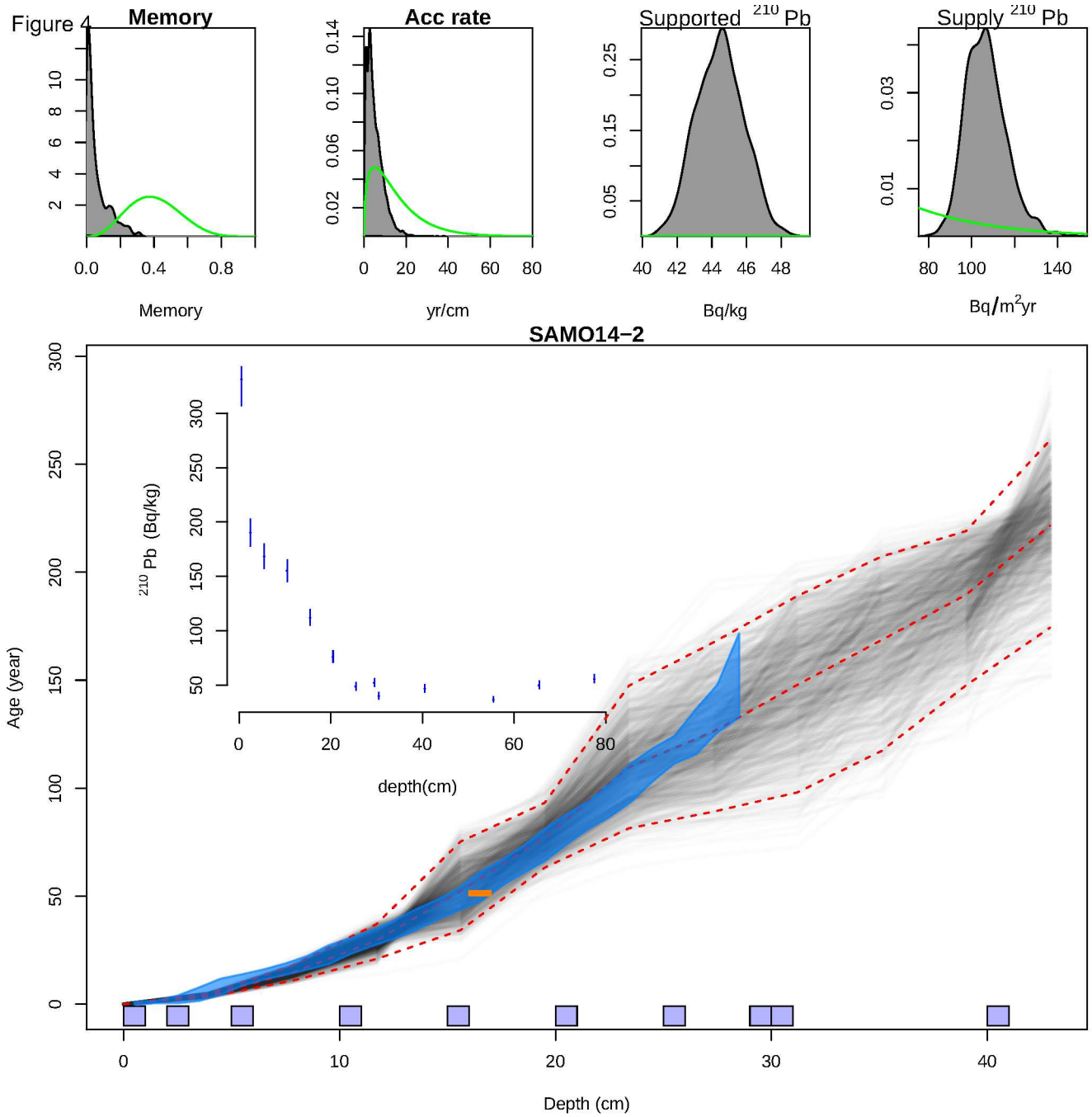
Memory
Acc rate
Supported 210 Pb
Supply 210 Pb
Memory
yr/cm
Bq/kg
Bq/m2yr
SAMO14−2
Age (year)
210 Pb (Bq/kg)
depth(cm)
Depth (cm)

Figure 5

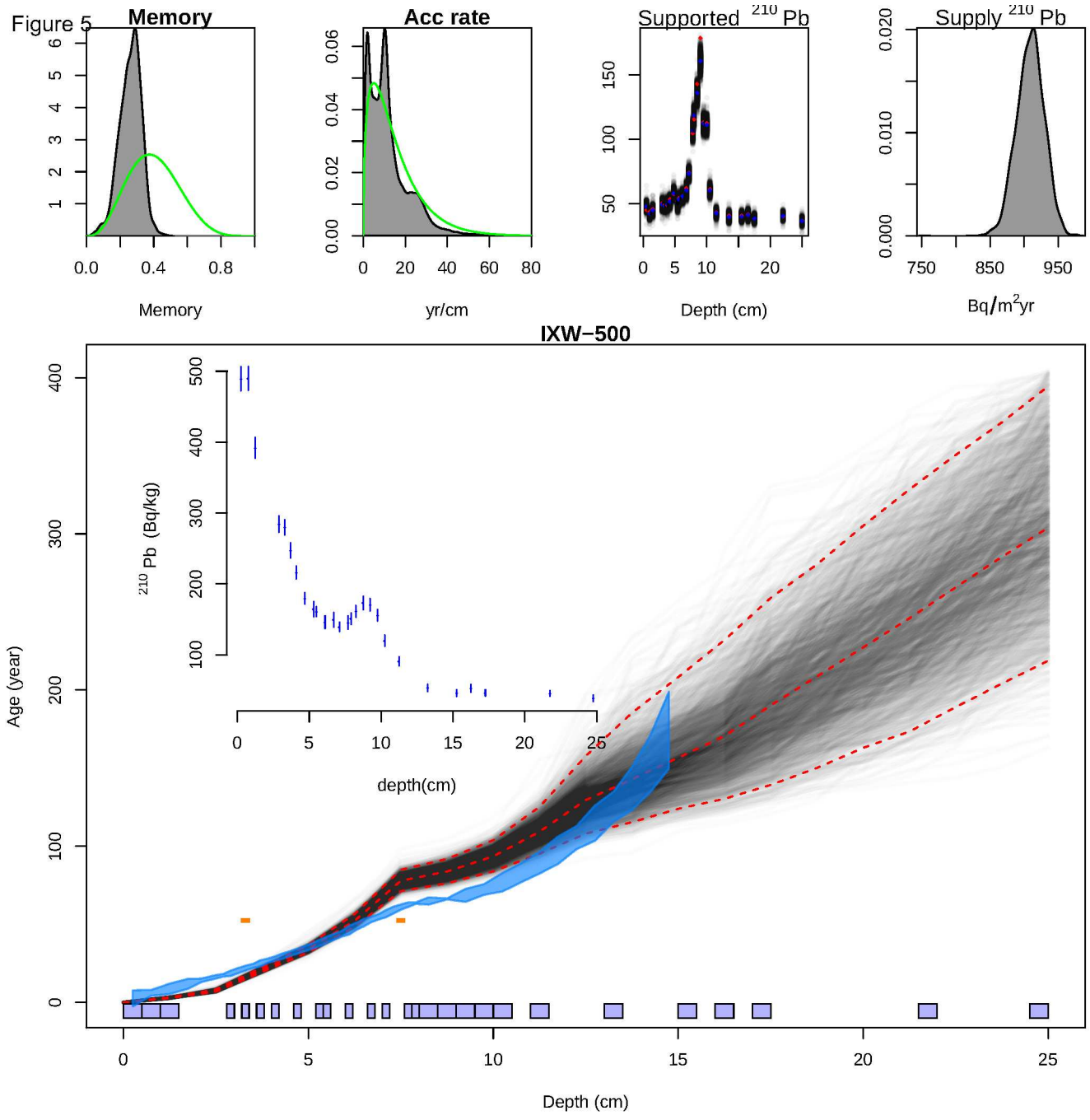
Memory
Memory
Acc rate
yr/cm
Supported 210 Pb
Depth (cm)
Supply 210 Pb
Bq/m2yr
IXW−500
Age (year)
Depth (cm)
210 Pb (Bq/kg)
depth(cm)

Conflict of Interest

Declaration of interests

☒ The authors declare that they have no known competing financial interests or personal relationships that could have appeared to influence the work reported in this paper.

☐The authors declare the following financial interests/personal relationships which may be considered as potential competing interests:

Declarations of interest: none.

Data

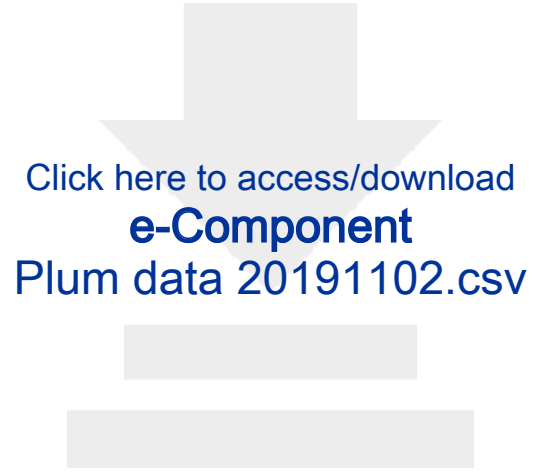

Click here to access/download
e-Component
Plum data 20191102.csv